

# Silicon Direct Opals

By Marta Ibisate, Dolores Golmayo, and Cefe López\*

Silicon is a relevant material with very diverse applications. This material allowed the development of the electronic technology and it is also very important in the fields of optoelectronics. Si has a very high refractive index, which is useful in some applications in photonics.<sup>[1]</sup> Porous Si (p-Si) has other important applications, such as light emission<sup>[2]</sup> and as sensor and catalyst.<sup>[3]</sup> Although initially p-Si was developed for use in light-emitting devices and optoelectronics, more recent interest has focused on exploring a range of biomaterial applications, due to its biocompatible nature and particularly since cells adhere to its surface. A recent application for p-Si is drug delivery, where drug molecules or proteins are loaded into the porous matrix and released into the body as the matrix degrades.<sup>[4,5]</sup> Since the discovery of luminescence from p-Si, research has focused on improving the room-temperature emission efficiency from this and other related silicon structures, and on understanding the mechanisms that give rise to such emission. Highly porous Si contains quantum-size crystalline structures responsible for the visible emission.<sup>[6,7]</sup> Particle size and surface chemistry influence the photoluminescence properties of p-Si. Recently, high quantum yields of up to 62% at wavelengths of about 789 nm were observed at room temperature.<sup>[8]</sup>

Amplification of light in a photonic crystal (PC) can be enhanced by localized defect states inside the photonic band-gap<sup>[9]</sup> or via modes with reduced group velocity at a photonic-band edge.<sup>[10]</sup> Room-temperature UV lasing in 3D PCs has been recently reported, where these structures consist entirely of optically active material.<sup>[11]</sup> Also, random lasing action has been recently demonstrated from randomly assembled monodisperse spheres and photonic glasses (PG) of polystyrene impregnated with a dye as the optical active medium.<sup>[12]</sup> In a PG, the multiple light scattering replaces the standard optical cavity of traditional lasers, and the interplay between gain and scattering determines the lasing properties. A PG can sustain scattering resonances over the gain-frequency window, and thus the lasing wavelength can be controlled by means of the diameter and refractive index of the spheres.<sup>[12,13]</sup> But the strength of these resonances is governed by the refractive index, a reason for which high refractive indices are dearly wanted.

Materials including nanocrystalline Si (nc-Si) have been prepared in the form of p-Si<sup>[14,15]</sup> or nc-Si embedded in a host matrix, mostly SiO<sub>2</sub>.<sup>[16]</sup> Recent results demonstrate that nc-Si

impregnated or implanted in artificial opals can have a significant effect on the photoluminescence emission of the material. This suggests that photonic structures could have potential applications in novel Si-based optoelectronic devices and structures,<sup>[17]</sup> even though neither Si nor p-Si have been used as building blocks in a 3D PC. A high-refractive-index material such as Si may be able to enhance resonances in PGs. Until now, it was impossible to synthesize monodisperse Si spheres in order to fabricate Si opals. Recently, Sandhage and coworkers<sup>[18]</sup> demonstrated that silica microstructures can be converted to nanometer-scale-p-Si microstructures under a low-temperature (650 °C) magnesiothermic reaction, while preserving the complex shape of the silica template, albeit with the introduction of nanometre-scale pores. Such direct low-temperature magnesiothermic conversion enables the synthesis of large numbers of 2D and 3D assemblies with well-controlled morphologies for catalytic/chemical, biological, optical, and other applications. Thin films of ordered mesoporous Si have been recently prepared by this method.<sup>[19]</sup>

The use of this method to obtain monodisperse Si spheres to produce a new building block class, exploring the new properties of this paradigmatic material, presents a great challenge. In the field of the light transport, it could be interesting to study how this monodisperse high refractive index changes light propagation. Since the optical properties of PCs are so clear signatures of periodicity, we used ordered arrangements (opals) to test the method.

In this work, we report a process to fabricate Si opals by magnesiothermic reduction of silica opals. The reduction of silica with gaseous Mg produces Si and magnesia keeping the structure unchanged. The magnesia selective etching with HCl solutions allow us to obtain opals made of p-Si spheres. The porous nature of these p-Si spheres (Si-air) involves a lower dielectric constant than that of Si. Some optical applications require high-refractive-index materials. To increase the refractive index of our spheres, the p-Si opal was treated by chemical vapor deposition (CVD) to infill the pore of the Si spheres.

X-ray diffraction, transmission electron microscopy (TEM), scanning electron microscopy (SEM), and optical spectroscopy have been performed in order to monitor the process and to analyze the crystal quality and composition of the samples.

The XRD diffraction data are shown in Figure 1. The samples substrate is (100)-oriented Si (single peak at  $2\theta = 69.13^\circ$ ), which does not interfere with the sample signal in the measurement range. Figure 1a shows the sample diffractogram after treatment with magnesium at 700 °C. This figure shows diffraction peaks corresponding to magnesia and Si. After selective etching with HCl, Figure 1b shows only peaks from Si, showing that removal of magnesia is complete. Figure 1c corresponds to the sample after the CVD process at 325 °C. No difference is observable between Figure 1b and c, due to the amorphous nature of Si

[\*] Prof. C. López, Dr. M. Ibisate, Dr. D. Golmayo  
Instituto de Ciencia de Materiales de Madrid (CSIC)  
and Unidad Asociada CSIC-U. Vigo  
C/Sor Juana Inés de la Cruz 3, 28049 Madrid (Spain)  
E-mail: cefe@icmm.csic.es

DOI: 10.1002/adma.200900188

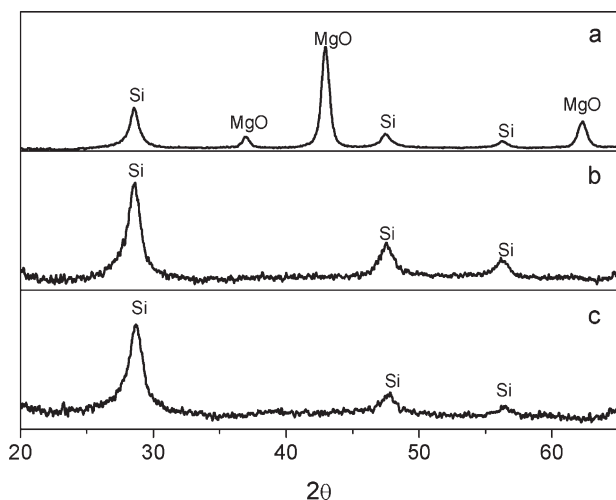


**Figure 1.** XRD: Diffractograms of the opals obtained after a) the magnesiothermic reduction, b) HCl etching, and c) CVD process.

growth at low temperatures. Scherrer analysis of the domain size from the diffraction-peak width indicates that the crystallite diameter is about 15 nm, in good agreement with the previous results of magnesiothermic reduction of silica.<sup>[18,19]</sup>

The spheres changed during the magnesiothermic reduction and CVD process were also analyzed by TEM (Fig. 2). The silica spheres (575 nm diameter) produced by the standard Stöber

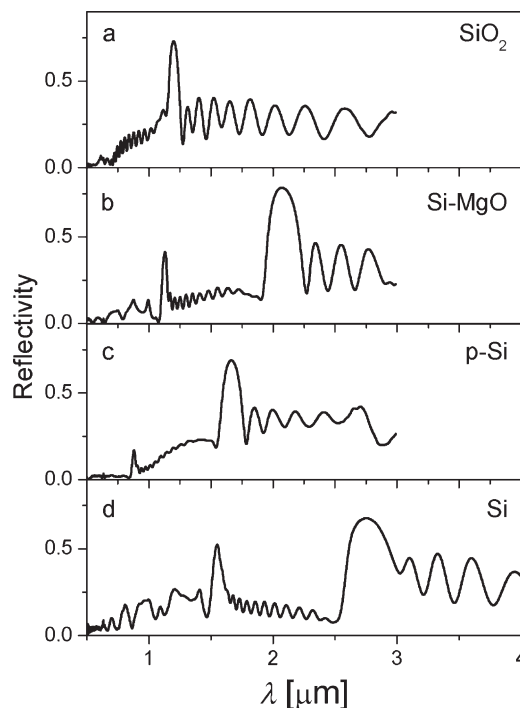


**Figure 3.** Reflectance for opals of a) SiO<sub>2</sub>, b) Si-MgO, c) p-Si, and d) nonporous Si spheres.

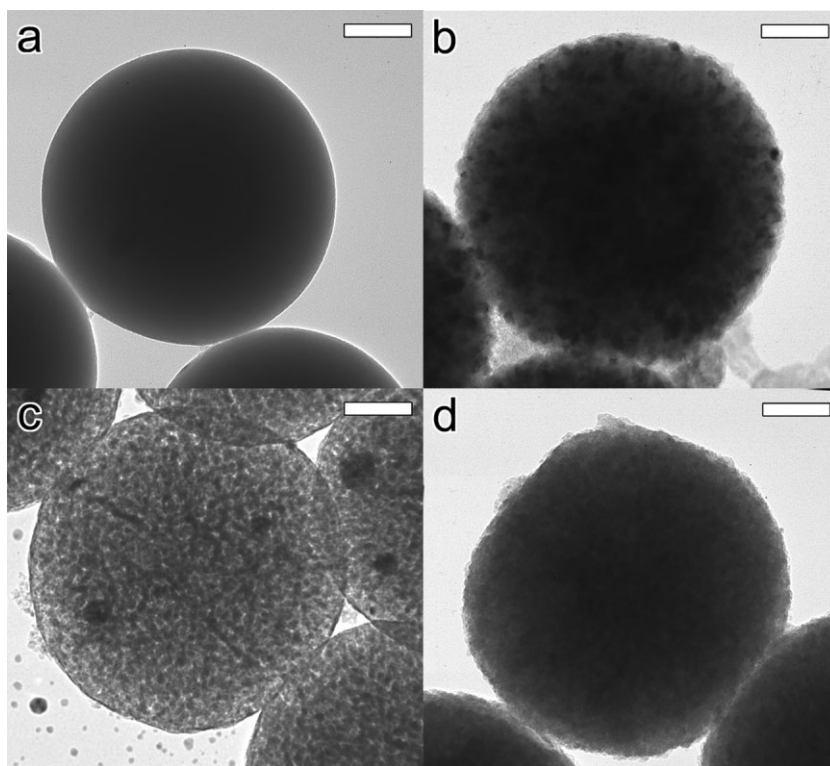


**Figure 2.** TEM images of a SiO<sub>2</sub> sphere a) before reduction, b) after magnesiothermic reduction, c) after HCl etching, and d) after CVD process. Scale bars: 120 nm.

method were treated at 600 °C to prevent the appearance of cracks<sup>[20]</sup> during the opal magnesiothermic reduction. After growth, the silica opals were treated at 700 °C to remove the silanol groups from the silica surface, in this way completely removing the water in the structure.<sup>[21]</sup> A TEM image of a silica sphere after the thermal treatments is shown in Figure 2a. The silica-sphere diameter was 550 nm. The magnesiothermic reduction process induces a size increase of the sphere due to the inclusion of Mg in form of MgO in the structure. The sphere size increases from 550 to 600 nm (Fig. 2b). In this image, the sphere nanocrystalline nature can be observed. Figure 2c shows the TEM image of the sphere after selective etching of MgO with HCl. The porous structure can be clearly observed. The spheres keep their shape and size from the previous step (600 nm). A TEM image after the CVD process at 325 °C is shown in Figure 2d. The sphere size is preserved. The preparation process for the TEM inspections produce fractures between spheres, and for this reason the particle in Figure 2d is not completely spherical.

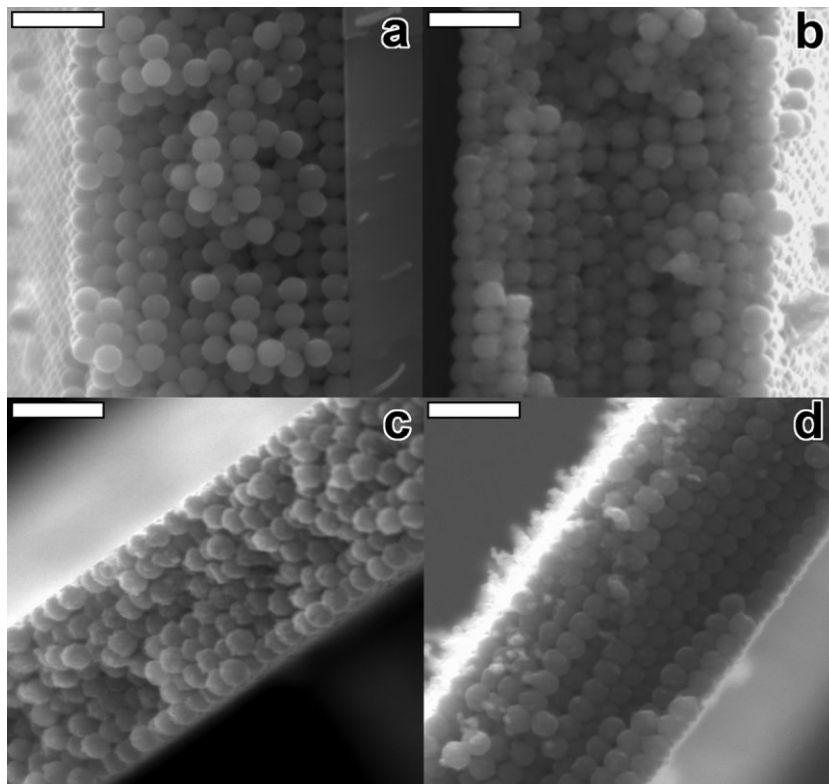
The transformation process has also been monitored by the optical reflectance at

near-normal incidence with respect to the (111) face-centered cubic (fcc) planes obtained with the help of an optical microscope and spectrometer (Fig. 3). The silica opal (Fig. 3a) spectrum shows a peak centred at 1196 nm, corresponding to the first photonic pseudogap opening at point L of the Brillouin zone. Since the opals are thin, Fabry–Perot oscillations can be seen along with the stronger Bragg peak. After magnesiothermic reduction (Fig. 3b), the Bragg peak shows a red shift due to the higher dielectric constant after the reduction process. The peak is now centered at 2070 nm. In Figure 3c, the Bragg peak can be observed at a lower wavelength (1662 nm), because of the refractive-index decrease after selective etching of MgO. The sample optical properties after the CVD process are shown in Figure 3d. This measurement was performed with a Cassegrain objective, since it was not possible to obtain a good measurement around 2900 nm with the refractive objective used for the previous measurement. A sizable red shift of the Bragg peak is observed, centered now at 2749 nm. In the whole process, the photonic band-gap shows a red shift of 1553 nm. In the four spectra, high-energy features are observable, guaranteeing that 3D periodicity and quality are preserved. These peaks are an unequivocal signature of lateral periodicity and stacking order.<sup>[22]</sup>

The order of the samples was also observed by SEM (Fig. 4). Figure 4a shows SEM images of the silica opal after the thermal treatment at 700 °C. In Figure 4b it is possible to observe how the ordered structure is preserved after the magnesiothermic reduction process even when this process induces a size increase in the spheres. The different particle size is observed clearer by TEM in Figure 2. The selective etching of MgO with HCl does not disturb the opal order, as observed in Figure 4c. An opal SEM image after CVD process at 325 °C is shown in Figure 4d.

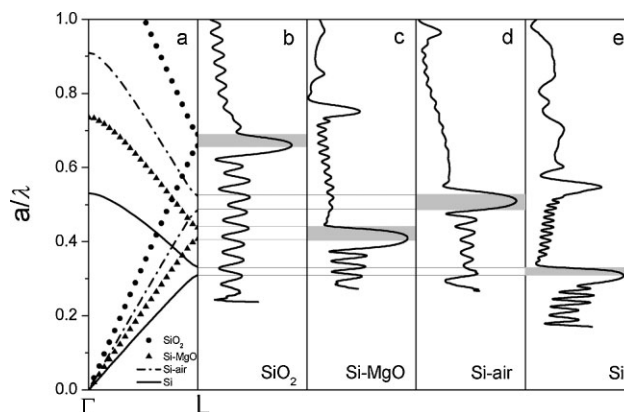
These results, both SEM inspections and optical reflectance, show that the opal structure is preserved upon magnesium reduction, in spite of the increasing size of the spheres. The diameter slightly larger than that of the original silica sphere implies some strain, but the optical quality of the opal is preserved, although parts of the opal can be detached from the substrate.

Figure 5 shows the reflectance spectra of opals formed by SiO<sub>2</sub>, Si-MgO, p-Si, and nonporous Si spheres, together with photonic band calculations performed using the MPB program, assuming that the SiO<sub>2</sub> dielectric constant is 1.90 (circles in Fig. 5a). The dielectric constant ( $\epsilon$ ) estimated for the Si-MgO sphere was 6.2 (triangles in Fig. 5a) assuming a 100% efficiency on the silica reduction. This estimation was achieved averaging the dielectric constant  $\epsilon = (n_1)^2 f_1 + (n_2)^2 f_2$ , where  $f$  is the volume fraction and  $n$  the refractive index. The volume fractions used, calculated from the molar volumes (11.20 mL/mol for MgO and 12.06 mL/mol for Si) were 0.65 for MgO and 0.35 for Si, and the refractive index



**Figure 4.** SEM images of a SiO<sub>2</sub> sphere a) before and b) after magnesiothermic reduction, c) after HCl etching, and d) after CVD process. Scale bars: 2 μm.

1.72 for MgO and 3.5 for Si. The dielectric constants used for the Si particles were 4.94 (65% of volume is air) and 12.5 for the porous (dashed-dotted line in Fig. 5a) and nonporous (solid line in Fig. 5a) particles, respectively. A good agreement between experimental data and theoretical calculations can be observed. The reflectance spectrum of the opal composed of nonporous Si



**Figure 5.** Reflectance spectra of a) SiO<sub>2</sub>, b) Si-MgO, c) p-Si, and d) nonporous Si opals, together with the a) corresponding photonic band calculations for SiO<sub>2</sub> (circles), Si-MgO (triangles), p-Si (dashed-dotted line), and nonporous Si (solid line) opals. Gray boxes indicate the corresponding photonic pseudogaps, and are a guide for the eye.

spheres (Fig. 5e) is broader than was expected from the theoretical predictions. This is due to the use of the Cassegrain objective. In this case, the incidence is not perfectly normal to the (111) fcc facet, because the objective collects a solid angle contained between  $27^\circ$  and  $43^\circ$  off normal.

In summary, we report here the use of magnesiothermic reduction and CVD to obtain opals formed by monodisperse Si spheres. XRD shows the formation of nc-Si after magnesiothermic reduction. TEM shows the porous structures of the p-Si spheres, and the infilling of these pores when the opal is post-infilled with Si by CVD. SEM shows that the ordered structure is preserved during the whole process.

This method allows the fabrication of porous and nonporous Si opals whose quality is proved by the optical properties. This is the only method that allows production of monodisperse spheres with a refractive index as high as 3.5, opening the possibility to new highly scattering monodisperse sphere-based materials.

## Experimental

Silica spheres were produced by the standard Stöber method. Prior to the assembly of the opal, silica spheres as dry powders were heat treated in order to prevent the appearance of cracks [23] in the opals during the subsequent dehydroxylation and infiltration processes. Silica powder was treated at  $600^\circ\text{C}$  at atmospheric pressure for 72 h, and then sonicated and dispersed in ethanol (3 wt%). Silica spheres were arranged by the vertical-deposition method to form thin artificial opals, which were used as templates for further processing. Si was used as substrate.

After growth, the opals were treated at  $700^\circ\text{C}$  to remove the silanol groups from the silica surface [21], completely removing the water of the structure. The magnesiothermic reduction of the silica opal was carried out in a stainless steel reactor composed of two chambers separated by 10 cm with CF format flanges. Magnesium powder (0.085 g) was placed in one chamber and around  $1\text{ cm}^2$  silica opal was placed in the other one; the reactor was then sealed under an Argon (4N) atmosphere in a glove bag. The reactor was introduced into a muffle furnace, ramped to  $700^\circ\text{C}$  in 1.5 h, and then held at this temperature for 2 h. The Si-MgO opal was then immersed in an HCl solution (1 M) for 6 h, removing the magnesia and leaving an opal of porous spheres of Si.

Finally, the porous Si opal was treated by CVD using disilane ( $\text{Si}_2\text{H}_6$ ) gas as a precursor (100 Torr, 1 Torr = 133.32 Pa). The deposition temperature was  $325^\circ\text{C}$  and reaction time was 12 h.

The X-ray powder diffraction study was carried out using a D8 Advance of Bruker using Cu K $\alpha$  radiation and a Lynx Eye detector.

The TEM and SEM images were obtained using a JEOL 2000 FX II and a Zeiss DSM 960, respectively.

Optical characterization was performed using a Fourier-transform infrared spectrometer, IFS 66S from Bruker, with an IR microscope attached.

## Acknowledgements

This work was partially funded by the Spanish Ministry of Science and Education under contract MAT2006-09062 and Consolider NanoLight.es CSD2007-0046, the EU under contract IST-511616 NoE PHOREMOST. M.I. is a Ramón y Cajal researcher. This work used the Transmission Electronic Microscopy and the X-ray diffraction facilities at the Instituto de Ciencia de Materiales de Madrid (CSIC), and the Scanning Electronic Microscopy facility at the Centro de Ciencias Medioambientales (CSIC).

Received: January 16, 2009

Revised: February 11, 2009

Published online: May 7, 2009

- [1] H. S. Sözüer, J. W. Haus, R. Inguva, *Phys. Rev. B* **1992**, *45*, 13962.
- [2] L. T. Canham, *Appl. Phys. Lett.* **1990**, *57*, 1046.
- [3] J. L. Gole, S. Lewis, S. Lee, *Phys. Status Solidi A* **2007**, *204*, 419.
- [4] J. Salonen, V.-P. Lehto, *Chem. Eng. J.* **2008**, *137*, 162.
- [5] K. L. Jarvis, T. J. Barnes, A. Badalyan, P. Pendleton, C. A. Prestidge, *J. Phys. Chem. C* **2008**, *112*, 9717.
- [6] A. G. Cullis, L. T. Canham, *Nature* **1991**, *353*, 335.
- [7] A. G. Cullis, L. T. Canham, P. D. J. Calcott, *J. Appl. Phys.* **1997**, *82*, 909.
- [8] D. Jurbergs, E. Rogojina, L. Mangolini, U. Kortshagen, *Appl. Phys. Lett.* **2006**, *88*, 233116(1–3).
- [9] S. John, *Phys. Rev. Lett.* **1987**, *58*, 2486.
- [10] S. Nojima, *Jpn. J. Appl. Phys. Part 2*, **1998**, *37*, L565.
- [11] M. Scharrer, A. Yamilov, X. Wu, H. Cao, R. P. H. Chang, *Appl. Phys. Lett.* **2006**, *88*, 201103.
- [12] S. Gottardo, R. Sapienza, P. D. García, A. Blanco, D. S. Wiersma, C. López, *Nat. Photonics* **2008**, *2*, 429.
- [13] P. D. García, R. Sapienza, A. Blanco, C. López, *Adv. Mater.* **2007**, *19*, 2597.
- [14] A. G. Cullis, L. T. Canham, P. D. J. Calcott, *J. Appl. Phys.* **1997**, *82*, 909.
- [15] B. Gelloz, A. Kojima, N. Koshida, *Appl. Phys. Lett.* **2005**, *87*, 031107.
- [16] L. Pavesi, L. D. Negro, C. Mazzoleni, G. Franzo, F. Priolo, *Nature* **2000**, *408*, 440.
- [17] P. Janda, J. Valenta, J.-L. Rehspringer, R. R. Mafouana, J. Linnros, R. G. Elliman, *J. Phys. D* **2007**, *40*, 5847.
- [18] Z. Bao, M. R. Weatherspoon, S. Shian, Y. Cail, P. D. Graham, S. M. Allan, G. Ahmad, M. B. Dickerson, B. C. Church, Z. Kang, H. W. Abernathy, III, C. J. Summers, M. Liu, K. H. Sandhage, *Nature* **2007**, *446*, 172.
- [19] E. K. Richman, C. B. Kang, T. Brezesinski, S. H. Tolbert, *Nano Lett.* **2008**, *8*, 3075.
- [20] A. A. Chabanov, Y. Jun, D. J. Norris, *Appl. Phys. Lett.* **2004**, *84*, 3573.
- [21] M. D. Sacks, T. Y. Tseng, *J. Am. Ceram. Soc.* **1984**, *67*, 526.
- [22] X. Checoury, S. Enoch, C. Lopez, A. Blanco, *Appl. Phys. Lett.* **2007**, *90*, 161131.
- [23] A. A. Chabanov, Y. Jun, D. J. Norris, *Appl. Phys. Lett.* **2004**, *84*, 3573.